Stochastic resonance in RF SQUID with shunted ScS junction

O.G. Turutanov[a,*], V.A. Golovanevskiy[b], V.Yu. Lyakhno[a], V.I. Shnyrkov[a]

[a]*B.Verkin Institute for Low Temperature Physics and Engineering, NAS Ukraine, 47 Lenin Ave., Kharkov 61103, Ukraine*
[b]*Western Australian School of Mines, Curtin University, Kent St., Bentley, Perth Western Australia 6845*

Abstract

Using a point (superconductor-constriction-superconductor, ScS) contact in a single-Josephson-junction superconducting quantum interference device (RF SQUID) provides stochastic resonance conditions at any, arbitrary small, value of loop inductance and the contact critical current unlike SQUIDs with more traditional tunnel (superconductor-insulator-superconductor, SIS) junctions. This is due to an unusual potential energy of the ScS RF SQUID which always has a barrier between two wells thus making the device bistable. This paper presents the results of the numerical simulation of stochastic dynamics of magnetic flux in the ScS RF SQUID loop affected by band-limited white Gaussian noise and low-frequency sine signal of small and moderate amplitude. The difference in stochastic amplification of the RF SQUID loops incorporating ScS and SIS junctions is discussed.

Keywords: stochastic resonance, RF SQUID, ScS Josephson junction
2010 MSC: 82D55, 65Z05, 70K30, 34F15
PACS: 05.40.Ca, 74.40.De, 85.25.Am, 85.25.Dq

1. Introduction

The sensitivity of superconducting quantum interference devices (SQUIDs) and their quantum analogues, SQUBIDs, has practically reached the quantum limitation [1–3]. However, with increase of the quantizing loop inductance up to $L \sim 10^{-9} - 10^{-10}$ H, the thermodynamic fluctuations lead to quick deterioration of the energy resolution. As shown earlier [4–8], sensitivity of magnetometers can be enhanced in this case by using stochastic resonance (SR). The SR phenomenon whose conception introduced in early 1980ths works [9–11] manifests itself in non-monotonic rise of a system response to a weak periodic signal when noise of certain intensity is added to the system. Owing to extensive studies of the last two decades, the stochastic resonance effect has been revealed in a variety of natural and artificial systems, both classical and quantum. The analytical approaches and quantifying criterions for estimation of the ordering due to of the noise impact were determined and described in reviews [12–14]. In particular, the sensitivity of a bistable stochastic system fed with a weak periodic signal can be significantly improved in the presence of thermodynamic or external noise that provides switching between the metastable states of the system. For example, it was experimentally proved [4] that the gain of a harmonic informational signal can reach 40 dB at certain optimal noise intensity in a SQUID with SIS (superconductor-insulator-superconductor) Josephson junction. Moreover, the stochastic amplification in SIS-based SQUIDs can be maximized at a noise level insufficient to enter the SR mode by means of stochastic-parametric resonance (SPR) effect [15] emerging in the system due to the combined action of the noise, a high-frequency electromagnetic field and the weak informational signal. An alternative way of enhancing the RF SQUID sensitivity is suppressing noise with strong (suprathreshold) periodic RF pumping of properly chosen frequency which results in better signal-to-noise ratio in output signal [16]. In the latter case switching between metastable states is mainly due to strong regular RF pumping unlike SR where the dominating switching mechanism is noise weakly perturbed [17].

---

*Corresponding author.
Email address:* `turutanov@ilt.kharkov.ua` (O.G. Turutanov)

In recent years the quantum point contacts (QPCs) with direct conductance have attracted strong interest from the point of view of both quantum channel conductance studies and building qubits with high energy level splitting. Currently, two types of point contacts are distinguished, depending on the ratio between the contact dimension d and the electron wave length $\lambda_F = h/p_F$: $d >> \lambda_F$ for a classical point contact [18] and $d \sim \lambda_F$ for a quantum point contact [19–21]. Practically, superconducting QPCs are superconductor-constriction-superconductor (ScS) contacts of atomic-size (ASCs). The critical currents of such contacts can take discrete values. The relation $I_s^{ScS}(\varphi)$ between supercurrent I_s^{ScS} and the order parameter phase φ in both classical and quantum cases at lowest temperatures ($T \to 0$) essentially differs [18, 20, 21] from the current-phase relation for a SIS junction described by the well-known Josephson formula $I_s^{SIS} = I_c \sin \varphi$. The corresponding potential energies in motion equations are therefore different as well.

When SIS junction is incorporated into a superconducting loop with external magnetic flux $\Phi_e = \Phi_0/2$ (where $\Phi_0 = h/2e \approx 2.07 \cdot 10^{-15}$ Wb is magnetic flux quantum) piercing the loop, its current-phase relation $I_s^{SIS}(\varphi)$ leads to formation of a symmetric two-well potential energy $U^{SIS}(\Phi)$ of the whole loop that principally enables the SR dynamics only for $\beta_L = 2\pi L I_c/\Phi_0 > 1$. β_L is dimensionless non-linearity parameter sometimes called the main SQUID parameter. In contrast, the potential energy $U^{ScS}(\Phi)$ of a superconducting loop with QPC always has the barrier with a singularity at its top, and two metastable current states of the loop differed by internal magnetic fluxes Φ can be formally achieved at any vanishingly low $\beta_L << 1$. In the quantum case, the most important consequences of the "singular" barrier shape are the essential rise of macroscopic quantum tunneling rate and the increased energy level splitting in flux qubits [2, 3].

In the classical limit, SR dynamics of the superconducting loop with ScS Josephson contact and non-trivial potential $U^{ScS}(\Phi)$ would differ substantially from the previously explored [4–6, 8] case of the SIS junction and would be much alike the 4-terminal SQUID dynamics [7]. In present work a numerical analysis is given of stochastic amplification of weak low-frequency harmonic signals in a superconducting loop broken by ScS Josephson junction at low temperatures $T << T_c$. Specific focus is giving to low critical currents, i.e. rather high-impedance contacts (ASCs) when $\beta_L = 2\pi L I_c/\Phi_0 < 1$.

2. ScS junction loop model and numerical computation technique

The stochastic dynamics of magnetic flux in a RF SQUID loop (inset in Fig. 1a) was studied by numerical solution of the motion equation (Langevin equation) in the resistively shunted junction (RSJ) model [22]:
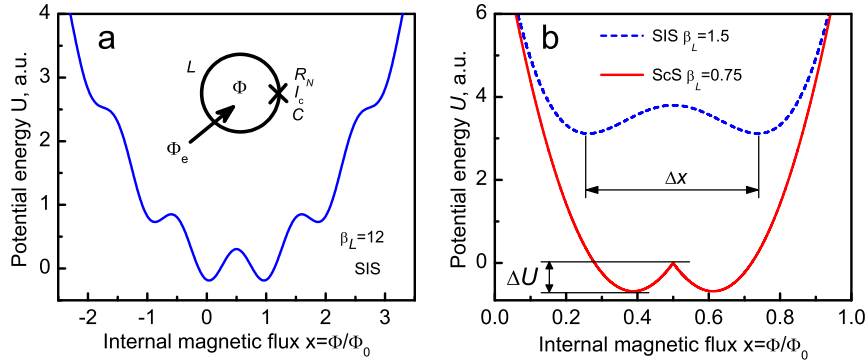

Figure 1: (Color online) (a) Potential energy U^{SIS} of SIS-junction-based RF SQUID loop with large non-linearity parameter $\beta_L = 12$ vs. normalized internal magnetic flux x. Inset is the RF SQUID loop schematic. (b) Potential energies of RF SQUIDs with SIS junction ($\beta_L = 1.5$) and ScS junction ($\beta_L = 0.75$) vs. normalized internal magnetic flux x. The barrier heights ΔU in both SQUIDs are approximately equal at chosen values of β_L. Fixed magnetic flux $\Phi_e = \Phi_0/2$ ($x_e = 1/2$) is applied to symmetrize the potential.

$$LC\frac{d^2\Phi(t)}{dt^2} + \frac{L}{R}\frac{d\Phi(t)}{dt} + L\frac{\partial U(\Phi, \Phi_e)}{\partial \Phi} = \Phi_e(t), \tag{1}$$

2

where C is the capacitance, R is the normal shunt resistance of the Josephson junction; L is the loop inductance; $\Phi(t)$ is the internal magnetic flux in the loop; $U(\Phi, \Phi_e)$ is the loop potential energy, which is the sum $U(\Phi, \Phi_e) = U_M + U_J$ of magnetic energy of the loop and the coupling energy of the Josephson junction. Time-dependent external magnetic flux $\Phi_e(t)$ piercing the loop contains a constant and a variable, including noise, components. This equation is analogous of the motion equation for a particle of mass C moving in potential U with friction coefficient $\gamma = 1/R$. The junction coupling energy U_J is specific to its nature; we will consider the case of clean ScS contacts in the ballistic mode of the electron fly-through [18].

For both classical [18] and quantum [19–21] ScS point contacts with the critical current I_c, at arbitrary temperature T the current-phase relation reads

$$I_s^{ScS}(\varphi) = I_c \sin \frac{\varphi}{2} \, \tanh \frac{\Delta(T) \cos \frac{\varphi}{2}}{2k_B T}, \quad I_c(T) = \frac{\pi \Delta(T)}{eR}, \tag{2}$$

where $I_s^{ScS}(\varphi)$ is the supercurrent through the contact, $\Delta(T)$ is the superconducting energy gap (order parameter), φ is the difference between the order parameter phases at the contact "banks", k_B is Boltzmann constant, e is the electron charge, R is the normal contact resistance. In the limit $T = 0$ the expression (2) transforms into

$$I_s^{ScS}(\varphi) = I_c \sin \frac{\varphi}{2} \, \text{sgn} \, (\cos \frac{\varphi}{2}) \tag{3}$$

The potential energy of a superconducting loop broken by the ScS contact, $U^{ScS}(\Phi, \Phi_e)$, reads as

$$U^{ScS}(\Phi, \Phi_e) = \frac{(\Phi - \Phi_e)^2}{2L} - E_J^{ScS} \cos \left| \frac{\pi \Phi}{\Phi_0} \right|, \tag{4}$$

where $E_J^{ScS} = I_c \Phi_0 / \pi$ is the maximum coupling energy of the ScS Josephson contact.

To compare, the potential energy of a loop with a tunnel junction is [22]

$$U^{SIS}(\Phi, \Phi_e) = \frac{(\Phi - \Phi_e)^2}{2L} - E_J^{SIS} \cos \frac{2\pi \Phi}{\Phi_0}, \tag{5}$$

where $E_J^{SIS} = I_c \Phi_0 / 2\pi$ is the maximum coupling energy of the tunnel Josephson junction.

Reducing the fluxes by flux quantum Φ_0 : $x = \Phi/\Phi_0$, $x_e = \Phi_e/\Phi_0$, the potential energy - by $\Phi_0^2/2L$, and using the parameter β_L, Eqs. (4) and (5), can be rewritten as, correspondingly

$$u^{ScS}(x, x_e) = \frac{(x - x_e)^2}{2} - \frac{\beta_L}{2\pi^2} \cos |\pi x| \tag{6}$$

and

$$u^{SIS}(x, x_e) = \frac{(x - x_e)^2}{2} - \frac{\beta_L}{4\pi^2} \cos(2\pi x) \tag{7}$$

Reduced potential energy $u^{SIS}(x, x_e)$ of the loop with a tunnel junction has two or more local minima at $\beta_L > 1$ only. When the loop is biased by a fixed magnetic flux $\Phi_e = \Phi_0/2$ ($x_e = 1/2$), the two lowest minima become symmetric. This case is illustrated in Fig. 1a for large value $\beta_L = 12$, for better illustrativeness.

The essential feature attributed to the potential energy $u^{ScS}(x, x_e)$ of RF SQUID with ScS contact is that the inter-well barrier with the singularity at its top keeps its finite height down to vanishingly small β_L and therefore small L and I_c. Fig. 1b shows the two-well potential of RF SQUID with the ScS contact at $\beta_L = 0.75 < 1$ (solid line) and, for comparison, the potential of the loop with the SIS junction (dashed line) with the same energy barrier height ΔU (see also Fig. 2a). The noise of thermal or any other origin causes switching between the metastable states corresponding to the minima of $U(\Phi)$. The average switching rate r_{sw} (of transition from a metastable state to another one) for white Gaussian noise with the intensity D and high barriers ($\Delta U/D \gg 1$) is estimated by well-known Kramers rate r_K [23]

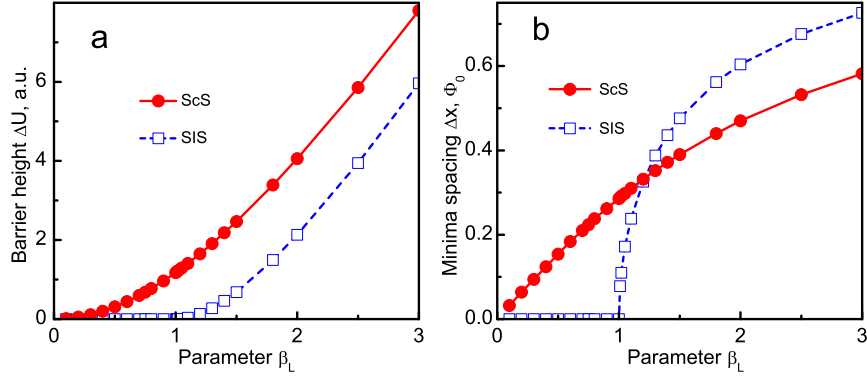$$r_{sw}^{smooth} = r_K = \frac{\omega_0 \, \omega_b}{2\pi \gamma} \, \exp(-\Delta U/D) \tag{8}$$

3

Figure 2: (Color online) (a) Energy barrier height ΔU and (b) spacing Δx between the potential energy minima vs. parameter β_L for RF SQUIDs with ScS and SIS Josephson junctions.

for parabola wells and smooth parabola barrier, which is almost the case for SIS-SQUID potential. Here $\omega_0 = [U''_\Phi(x_{bottom})/C]^{1/2}$ and $\omega_b = [U''_\Phi(x_{top})/C]^{1/2}$ are angular frequencies of small-amplitude oscillations near the bottom of the well and the top of the barrier, correspondingly, defined by the potential curvature in these points; γ is the damping constant.

Meanwhile, for parabola wells and sharp barrier that is close to the ScS SQUID potential shape, especially at low non-linearity parameter β_L, the switching time is given by formula (5.4) in [24], which in our terms will read as:

$$r_{sw}^{sharp} = \sqrt{\pi}\frac{\gamma(\Delta x)^2}{8\Delta U}\sqrt{\frac{D}{\Delta U}}\exp(-\Delta U/D) \qquad (9)$$

For the thermal noise, $D = k_B T$. In this work we do not presume any specific nature of the noise, however, considering it white Gaussian. The sole limitation we impose is setting an upper cut-off frequency f_c for the noise band which does not exceed the reversal time of the flux relaxation in the loop $1/\tau_L = R/L$ to provide the adiabatic mode for the SQUID operation. Previous estimations [8, 15] following from the numerical simulation show that a "reasonable" value for f_c can be chosen so that its further increase does not practically affect the results of the calculations. Usually $f_c \sim (10^3 - 10^4)f_s$ is high enough where f_s is the signal frequency. Adding small periodic signal with frequency f_s to the external flux Φ_e on the noise background enables stochastic resonance dynamics of a particle in the bistable potential when the SR condition fulfils:

$$r_{sw} \approx 2f_s \qquad (10)$$

For typical experimental parameters, $L \approx 3 \cdot 10^{-10}$ H, $C \approx 3 \cdot 10^{-15}$ F, $R \approx 1 - 10^2$ Ohm, $I_c \approx 10^{-5} - 10^{-6}$ A and $\beta_L = 0.1 - 3$, we estimate McCumber parameter accounting for the capacitance to be low enough: $\beta_C = 2\pi R^2 I_c C/\Phi_0 < 1$. In this case (aperiodic, or overdamped, oscillator) the motion is non-oscillatory, and therefore the first term with second derivative in Equation 1 can be neglected. Note that a contact with resistance $R \sim 100$ Ohm is close to ASC since the number of conducting channels (atomic chains) is small but the considered situation, even at low temperatures, remains classical one because of strong dissipation. The low signal frequency $f_s \sim 1 - 10$ Hz $<< 1/\tau_L$ and the upper-limited noise frequency band (quasi-white noise) with cut-off frequency $f_c \sim 10^4$ Hz $<< 1/\tau_L$ make the problem adiabatic, as noted above, and allows to attribute all time dependence to the potential energy in Equation (1):

$$\tau_L\frac{dx}{dt} + \frac{\partial U(x,t)}{\partial x} = 0 \qquad (11)$$

For the case of an ScS contact, by substituting Equation (6) in Equation (11), we get

$$\frac{dx}{dt} = \frac{1}{\tau_L}\{x_e(t) - x + \frac{\beta_L}{2\pi}\sin(\pi x) \cdot sgn[\cos(\pi x)]\}, \qquad (12)$$

and for an SIS junction, taking into account Equation (7), Equation (11) reads as

4

$$\frac{dx}{dt} = \frac{1}{\tau_L}[x_e(t) - x + \frac{\beta_L}{2\pi}\sin(2\pi x)] \tag{13}$$

The external magnetic flux $x_e(t)$ is the sum of the fixed bias flux $x_{dc} = 0.5$, the useful signal $x_{ac} = a\sin 2\pi f_s t$ and the noise flux x_N. Theoretically, the noise is assumed to be δ-correlated, Gaussian-distributed, white noise: $x_N = \xi(t)$, $\langle \xi(t)\xi(t - t')\rangle = 2D\delta(t - t')$. During numerical simulation it is emulated by a random-number generator with Gaussian distribution, variance $D = \sigma^2$ and repetition period of about 2^{90}. When solving the equation in a finite-difference approximation, the sampling frequency is 2^{16} which is equivalent to noise frequency band ~ 32 kHz. This allows us to consider the noise to be quasi-white for stochastic amplification of the signals with frequency $f_s = 1 - 10$ Hz.

Equations (12) and (13) were solved by Heun algorithm modified for stochastic equations [25, 26]. 10 to 50 runs were made to obtain 16-second time series with different noise realizations. They underwent then fast Fourier transform (FFT), and the resulted spectral densities $S_\Phi(\omega)$ of output signal (internal flux in the loop) were averaged. In this work we use the spectral amplitude gain of the weak periodic signal as the SR quantifier defined as the ratio of spectral densities of output and input magnetic fluxes:

$$k(\omega) = S^{1/2}_{\Phi out}(\omega)/S^{1/2}_{\Phi in}(\omega) \tag{14}$$

3. Numerical simulation results and discussion

The energy barrier height ΔU, as follows from Equations (6) and (7), is determined by β_L and is different for the cases of ScS and SIS junctions (Fig. 2a). As can be seen, in the loop with SIS junction (referred to as SIS SQUID) the two-well potential with two metastable states needed to prepare conditions for stochastic amplification of a weak information signal exists only at $\beta_L > 1$ while it is finite for any β_L in the ScS SQUID. Both ΔU and D, being in exponent, are the core parameters to define switching rate r_{sw} (8), (9). For a specified frequency of a weak harmonic signal, the SR condition (10) requirement can be met by increasing the noise power. Meanwhile, the amplitude gain $k(\omega)$ of the small signal, according to the two-state theory [27], should depend on spacing Δx between the local minima of potential energy $U(x)$.

$$k(\omega) = \frac{r_{sw}(\Delta x)^2}{2D(4r_{sw}^2 + \omega^2)^{1/2}} \tag{15}$$

Fig. 2b shows Δx as a function of β_L for the ScS and SIS SQUIDs. It is obvious from Fig. 2b that both the spacing Δx^{ScS} between the potential energy minima and the barrier height ΔU^{ScS} tend to zero remaining finite when $\beta_L \to 0$. In contrast, for SIS SQUIDs ΔU^{SIS} and Δx^{SIS} vanish at $\beta_L = 1$.

Calculation of the small-signal gain with the same barrier height for both potentials, $\Delta U^{ScS} = \Delta U^{SIS}$, show that maximal gain for SIS SQUID is roughly twice higher than that of a SR amplifier based on ScS SQUID (Fig. 3a).

Maximal gain is obtained when SR condition (10) is met. After substituting (10) in (15) the gain becomes a function of only Δx and D. However, the obtained difference in the gain is less than could be derived from only the ratio of Δx^{ScS} to Δx^{SIS} because the gain maxima correspond to different optimal noise intensities $D_m = \sigma_m^2$ which depend on the potential shapes modifying switching rate r_{sw}. Using σ_m from Fig.3a to calculate gain ratio by formula (15), we get $k^{SIS}/k^{ScS} = 2.15$ versus experimental value of 2.37. This is good enough taking into account the simplicity of the two-state model. Fig.3b illustrates the alternative case when the minima spacing for both potentials are equal while the barriers are different. Unexpectedly, there is no agreement here between simulated and calculated gain ratios. Nevertheless, it should be stressed that despite lower gain in ScS SQUID, the SR amplification in it is possible at very small critical currents (typical for ASCs) and low noise level (that may correspond to thermodynamic fluctuations at ultralow temperatures). Meanwhile, there is no amplification of weak informational signals in SIS SQUIDs for all $\beta_L < 1$.

Fig. 4 displays a set of SR gain in ScS SQUID vs. noise intensity curves for several $\beta_L < 1$ and corresponding amplitude Fourier spectra of output signal normalized by Fourier spectra of input signal thus showing the spectral amplification $k(f)$. It is seen that, for sine signal of small amplitude ($a = 10^{-3}$) the system response remains linear even for small $\beta_L = 0.1$ that is indicated by no sign of third harmonic in the output spectrum (even harmonics are absent due to the potential symmetry). The latter case corresponds to millikelvin temperature range for real devices.
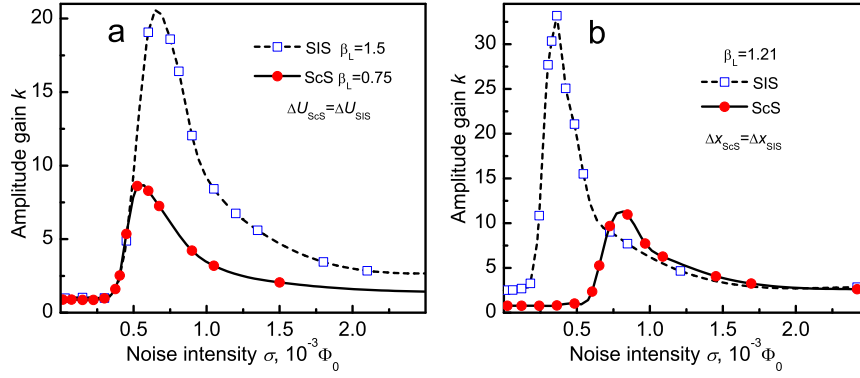
Figure 3: (Color online) Amplitude gain k of sine signal in RF SQUIDs with ScS and SIS junctions vs. noise amplitude $\sigma = D^{1/2}$. β_L parameters are chosen so that (a) the potential barriers ΔU in both SQUIDs were equal; (b) the minima spacing Δx in both SQUIDs were equal. Signal amplitude $a = 0.001$ and frequency $f_s = 10$ Hz

.

Although it is obvious that the detected spectrum is clearer at lower temperature because of smaller noise background, additionally the signal gain also turns out to be high enough at $\beta_L = 0.1$.
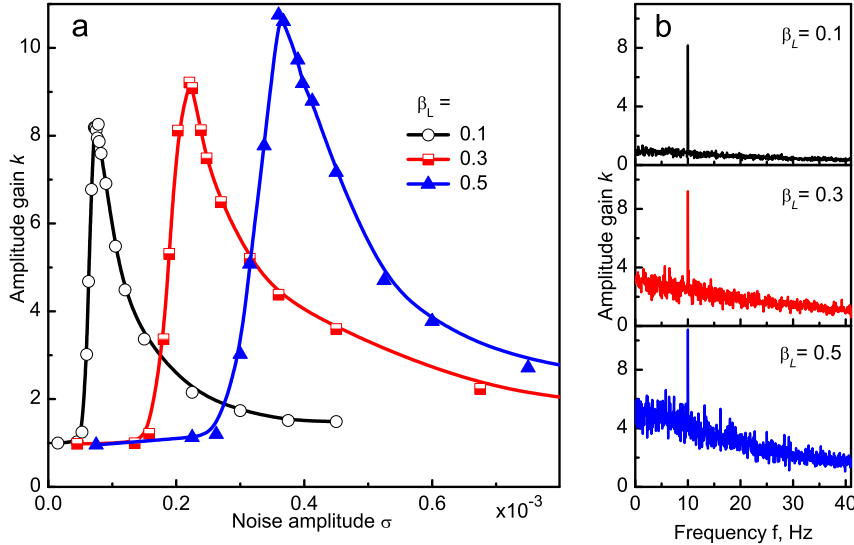

Figure 4: (Color online) (a) Amplitude gain k of sine signal in RF SQUID with ScS junction for various $\beta_L = 0.1, 0.3, 0.5$ vs. noise amplitude $\sigma = D^{1/2}$. (b) Spectral gains $k(f)$ for the same values of β_L as in panel (a) and noise levels corresponding to the peak of each curve in panel (a). Signal amplitude $a = 0.001$ and frequency $f_s = 10$ Hz.

The effect of degradation of stochastic amplification in ScS SQUID with the signal amplitude increase is shown in Fig. 5. The higher the signal amplitude, the smaller the signal gain, while third harmonic (and other odd ones) in the output Fourier spectrum become visible for $a = 3 \cdot 10^{-3}$ and 10^{-2} (even harmonics are absent because of the potential symmetry), thus the amplification becomes markedly non-linear. Since signal-to-noise ratio (SNR) enhancement in output signal is hardly expected for moderate-to-subthreshold signals on the background of rather weak noise (associated with small β_L) [28], the linear amplification is more suitable in this case. Therefore, the weakest signals are stochastically amplified by ScS SQUID most effectively.

The maximum stochastic gain for a weak ($a = 0.001$) low-frequency ($f_s = 10$ Hz) sine signal in both types of SQUIDs is presented in Fig. 6a vs. the main SQUID parameter $\beta_L = 0.1 - 3$. Formal divergence of the signal gain
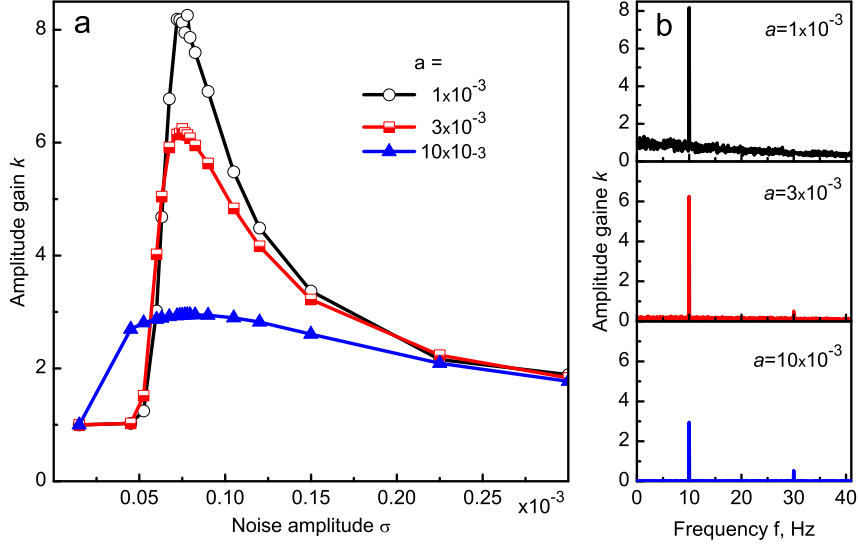
Figure 5: (Color online) (a) Amplitude gain of sine signals with various amplitudes a in ScS RF SQUID vs. noise amplitude $\sigma = D^{1/2}$. Spectral amplitude gain $k(f)$ for the same a as in panel (a) and noise levels corresponding to the gain curves maxima in panel (a). The signal frequency $f_s = 10$ Hz, parameter $\beta_L = 0.1$

.

obtained for SIS SQUID at $\beta_L = 1$ will be smeared by noise in real experiments. Besides, as an additional analysis shows, the non-linear signal distortions drastically rise and the dynamic range narrows in the region in the vicinity of $\beta_L = 1$. For the ScS SQUID, the dependence of the signal SR gain on the main parameter β_L has no distinctive features within a wide range of β_L including $\beta_L < 1$. The narrowing of the dynamic range and rise of the non-linear distortion is observed at $\beta_L << 1$ alike SIS-SQUID-based amplifiers near $\beta_L = 1$ due to vanishingly small potential barrier. Fig. 6b presents the optimal noise levels where maximum gain is reached as a function of parameter β_L. As expected, the optimal noise levels depend mostly on the height of the barrier between the two metastable current states. It follows from the obtained results that in small signal approximation when the response is supposed to be linear, SIS SQUIDs should be used as SR amplifiers at $\beta_L \geq 1$, while ScS SQUIDs are suitable for small critical currents and/or inductances associated with flux qubits, that is for $\beta_L < 1$.
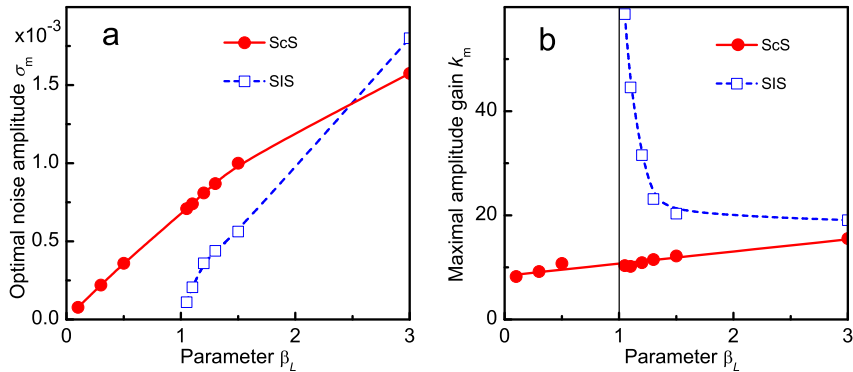

Figure 6: (Color online) (a) Maximum gain k_{max} and (b) optimal noise amplitude σ_m for ScS and SIS RF SQUIDs vs. parameter β_L. The signal frequency $f_s = 10$ Hz and amplitude $a = 0.001$.

7

4. Conclusion

In the given work the noise-induced stochastic amplification of weak informational signals at low temperatures $T \ll T_c$ in RF SQUIDs containing ScS contacts (QPCs) is considered. It is shown that SR amplification of weak sine signals emerges at any, vanishingly small, value of parameter β_L. This is due to an unusual shape of the potential barrier between the two metastable states with a singularity in its top and always finite height. It should be noted that there is no noise-induced re-normalization of the potential energy of ScS SQUID because the noise is band-limited. That justifies the use of the zero-temperature approximation.

Taking into account quantum corrections to the decay rate of the metastable current states in SR [29] can lead to essential modification of the dynamics and rise of SR gain. For example, as reported in paper [30], under some conditions the presence of the noise could enhance quantum correlation in superconducting flux qubits. With temperature rise up to T_c, SR dynamics of RF SQUID with QPC will change due to temperature dependence of the potential, $U^{ScS}(T)$ [31], tending, apparently, to that of the SIS SQUIDs.

It is worth noting that a discontinuous ("saw-like") current-phase relationship at $T = 0$ is also a characteristic of other types of Josephson contacts with direct conductance, e.g., 4-terminal microbridge junction and superconductor-normal metal-superconductor (SNS) junction that results in a singularity on the top of the barrier of the potential of such junctions [32, 33] and hence their stochastic dynamics should be similar to the behavior of RF SQUID with the considered ScS contact.

In addition, we would like highlight one important feature of SR. Even in the case when the SR effect in SQUID is considered as "stochastic filtration" [34], and no enhance in signal-to-noise ratio is anticipated as compared to its "input" value [28], the SR effect has almost self-evident advantage over other amplification methods because it works directly inside the sensor, thus providing a kind of "first aid" to signal detection that we could call "Just-In-Place Amplification" unlike widely spread "On-Chip" technical solutions where amplification is carried out in a separate unit situated near the sensor on a common substrate.

Acknowledgements

References

References

[1] M.B. Ketchen, J.M. Jaycox, Appl. Phys. Lett. 40 (1982) 736.
[2] V.I. Shnyrkov, A.A. Soroka, and O.G. Turutanov, Phys. Rev. B 85 (2012) 224512.
[3] V.I. Shnyrkov, A.A. Soroka, A.M. Korolev, and O.G. Turutanov, Low Temp. Phys. 38 (2012) 301.
[4] R. Rouse, Siyuan Han, and J.E. Lukens, Appl. Phys. Lett. 66 (1995) 108.
[5] A.D. Hibbs, A.L. Singsaas, E.W. Jacobs, A.R. Bulsara, J.J. Bekkedahl et al., J. Appl. Phys. 77 (1995) 2582.
[6] A.D. Hibbs and B.R. Whitecotton, Appl. Supercond. 6 (1998) 495.
[7] O.G. Turutanov, A.N. Omelyanchouk, V.I. Shnyrkov, Yu.P. Bliokh, Physica C 372-376 (2002) 237.
[8] A.M. Glukhov, O.G. Turutanov, V.I. Shnyrkov, and A.N. Omelyanchouk, Low Temp. Phys. 32 (2006) 1123.
[9] R. Benzi, A. Sutera, and A. Vulpiani, J. Phys. A14 (1981) L453.
[10] J.-P. Eckmann, L. Thomas, and P. Wittwer, J. Phys. A 14 (1981) 3153.
[11] C. Nicolis and G. Nicolis, Tellus 33 (1981) 225.
[12] L. Gammaitoni, P. Hänggi, P. Jung, and F. Marchesoni, Rev. Mod. Phys. 70 (1998) 223.
[13] V.S. Anishchenko, A.B. Neiman, F. Moss, and L. Schimansky-Geier, Phys. Usp. 42 (1999) 7.
[14] T. Wellens, V. Shatokhin and A. Buchleitner, Rep. Prog. Phys. 67 (2004) 45.
[15] O.G. Turutanov, V.I. Shnyrkov, and A.M. Glukhov, Low Temp. Phys. 34 (2008) 37.
[16] A.L. Pankratov, Phys. Rev. E 65 (2002) 022101.
[17] A.L. Pankratov, Phys. Rev. B 68 (2003) 024503.
[18] I.O. Kulik and A.N. Omelyanchouk, Sov. J. Low Temp. Phys. 4 (1978) 142.
[19] N. Agraït, A.L. Yeyati, and J.M. van Ruitenbeek, Phys. Rep. 377 (2003) 81.
[20] C.W.J. Beenakker and H. van Houten, Phys. Rev. Lett. 66 (1991) 3056.
[21] C.W.J. Beenakker and H. van Houten, The superconducting quantum point contacts, in Nanostructures and Mesoscopic Systems, ed. by W.P. Kirk and M.A. Reed (Academic, New York, 1992), p. 481 (arXiv:cond-mat/0512610).
[22] A. Barone and G. Paterno, Physics and Applications of the Josephson Effect, Wiley, New York 1982.
[23] H.A. Kramers, Physica 7 (1940) 284.

[24] A.N. Malakhov, A.L. Pankratov, Physica A 229 (1996) 109.

[25] J.L. Garcia-Palacios, Introduction to the theory of stochastic processes and Brownian motion problems, arXiv:cond-mat/0701242.

[26] Peter E. Kloeden, Eckhard Platen, Numerical Solution of Stochastic Differential Equations, 632 pp., Springer, 1992.

[27] B. McNamara, K. Wiesenfeld, Phys.Rev. A 39 (1989) 4854.

[28] P. Hänggi, M.E. Inchiosa, D. Fogliatti, and A.R. Bulsara, Phys. Rev. E 62 (2000) 6155.

[29] M. Grifoni, L. Hartmann, S. Berchtold, and P. Hänggi, Phys. Rev. E 53 (1996) 5890.

[30] A.N. Omelyanchouk, S. Savel'ev, A.M. Zagoskin, E. Il'ichev, F. Nori, Phys. Rev. B 80 (2009) 212503.

[31] V.A. Khlus, Sov. J. Low Temp. Phys. 12 (1986) 14.

[32] R. de Bruyn Ouboter, A.N. Omelyanchouk, Superlattices and Microstructures, 25 (1999) 1005.

[33] I.O. Kulik, Low Temp. Phys. 30 (2004) 528.

[34] Yu.L. Klimontovich, Physics-Uspekhi 42 (1999) 37.